Structure and Dynamic Properties of Molten Lanthanum Tribromide

Yoshihiro Okamoto and Toru Ogawa

Japan Atomic Energy Research Institute (JAERI), Tokai-mura, Naka-gun, Ibaraki-ken, 319-1106, Japan

Z. Naturforsch. **54a,** 91–94 (1999); received November 27, 1998

The structure of molten $LaBr_3$ was investigated by X-ray diffraction and molecular dynamics simulations. It was found that the short range structure of molten $LaBr_3$ is very similar to that of molten $LaCl_3$, except for some structural features such as interionic distances based on the difference of anion sizes. In the MD simulation, the shear viscosity of molten $LaBr_3$ was estimated from the structurally-optimized MD calculations.

Key words: Molten Salt; Rare Earth Halide; X-ray Diffraction; Molecular Dynamics.

1. Introduction

Molten salt technology may be used in nuclear fuel cycles based on pyrochemical processes [1] and the transmutation of actinides with a proton accelerator [2]. Presently, however, little is known about the physical properties of molten actinide chlorides.

We have studied the structure of molten rare earth and uranium trichlorides by using high-temperature X-ray diffraction (XRD) [3]. Information concerning the chloride ion, however, is insufficient in the XRD analysis became the scattering from chlorine is weaker than that from the rare earths and uranium. In the present work, structure of molten $LaBr_3$, having a heavier anion than $LaCl_3$, was investigated by the XRD technique. The physical properties of solid $LaBr_3$ are rather similar to those of $LaCl_3$, as summarized in Table 1. Thus more detailed structural information for molten trihalides can be derived by comparing XRD of molten chloride and bromide.

2. Procedures

2.1. High-temperature X-ray Diffraction

$LaBr_3$ and $LaCl_3$ were purified by a sublimation technique from the commercial products (99.9% purity). The samples were sealed in a quartz cell (0.5 mm thickness) under reduced pressure. The measurements were performed by using RINT2500TR (Rigaku corporation, Max. Power 18 kW) with an electric furnace. The temperature of molten $LaBr_3$ was 1150 K (mp. 1050 K). Also molten $LaCl_3$ was studied for comparison. Mo $K\alpha$ radiation (0.071069 nm wavelength) of 12.5 kW (50 kW, 250 mA) was used. The reduced intensity function $Q\,i(Q)$ and radial distribution function (RDF) $G(r)$ were obtained after some corrections and normalization as described in [4].

Table 1. Physical properties of $LaBr_3$ and $LaCl_3$.

Compound	Crystal type	Melting point (K)	Molar volume (cm^3/mol)	Electrical conductivity (S/m)	Shear viscosity (cP)
$LaBr_3$	UCl_3	1050	76.881	114.366	not reported
$LaCl_3$	UCl_3	1131	76.757	129.671 [a]	6.2242 [a]

All values are for 1150 K, except crystal structure.
[a] Values are based on extraporation.

$Q\,i(Q)$ can be obtained by the Debye scattering equation [4] with the three parameters interionic distance r_{ij}, correlation number n_{ij} and temperature factor b_{ij}:

$$Q\,i(Q) = \sum_{i=1}^{n} \sum_{j} n_{ij}\, f_i(Q)\, f_j(Q) \cdot \exp(-b_{ij}\, Q^2)\, \sin(Q\, r_{ij}) / r_{ij}\,, \qquad (1)$$

where $f_i(Q)$ is an atomic scattering factor of atom i. The structural parameters of the Debye scattering equation were determined by least square fitting to the experimental $Q\,i(Q)$.

2.2. Molecular Dynamics Simulation

A 1000 particle system (La: 250 and Br: 750) and the pair potential [5]

Reprint requests to Y. Okamoto; Fax: +81-29-282-5922.

$$\phi_{ij}(r) = \frac{n_1^2 z_i z_j e^2}{r} + n_2 b (f_i + f_j) \cdot \exp\left[\frac{\sigma_i + \sigma_j - r}{f_i + f_j}\right] + D_M \cdot \{\exp[-2\alpha(r - r_0)] - 2\exp[-\alpha(r - r_0)]\} \quad (2)$$

were used in the simulation.

The pair potential is a combination of the ionic Busing-type potential and the covalent Morse potential. z_i, σ_i and f_i are the electric charge, size parameter and repulsion constant of the ion i, respectively. n_1 corresponds to the ionicity and n_2 is an adjustable parameter of the repulsion term. In the present study, $n_1 = n_2$ was assumed for simplicity. In the third term (2), which corresponds to the Morse potential, $D_M = 0$, α, and r_0 are the dissociation energy, sharpness, and equilibrium distance of covalent bonding. The Morse potential was applied only to the nearest neighbor La–Br pair. In the fully ionic model, $n_1 = n_2 = 1$ and D_M. These parameters in (2) were determined to reproduce the experimentally obtained functions $Q\,i(Q)$ and $G(r)$. In [3, 6] the structure, thermodynamic and dynamic properties of molten $LaCl_3$ and UCl_3 were satisfactorily reproduced by using the above potential model.

The structural properties were obtained by accumulation of 50 000 ionic positions. The shear viscosity was calculated by the Kubo-type formula [7] from 250 000 steps. The step width was 2.0 fs. The calculations were mainly performed by the supercomputer VPP500/42 (Fujitsu) at JAERI using a vectorized and parallelized code. In a typical calculation for the 1000 particle system, a CPU time of 0.469 sec for each MD step was required in a single PE (processing element) and 0.248 sec in a 4 PE parallel system.

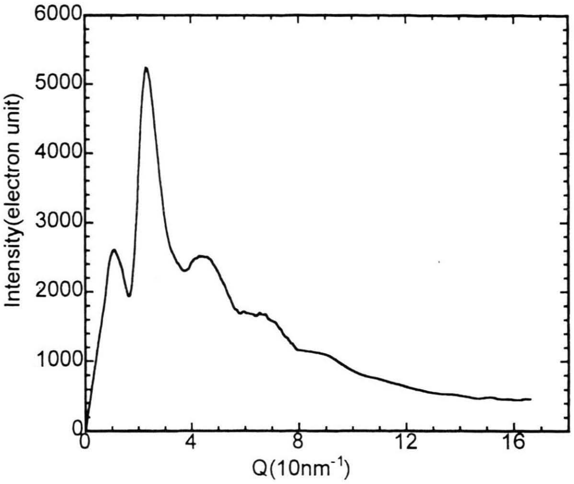

Fig. 1. Scattered X-ray intensity of molten $LaBr_3$ at 1150 K.

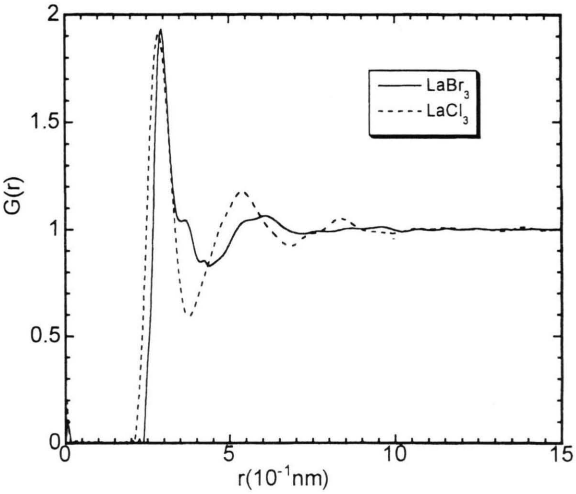

Fig. 2. Correlation functions $G(r)$ of molten $LaBr_3$ and $LaCl_3$ at 1150 K.

3. Results and Discussion

The observed scattered X-ray intensity of molten $LaBr_3$ is shown in Figure 1. A first sharp diffraction peak (FSDP) was observed around 10 nm^{-1}, as for many molten rare earth trichlorides [4, 8] and uranium trichloride [3]. This suggests that there is a medium range structural order also in molten $LaBr_3$. The correlation function $G(r)$ of $LaBr_3$ is shown in Fig. 2 together with that of $LaCl_3$. The shortest La^{3+}–Br^- distance was 0.295 nm (in the crystalline state it is 0.310 nm [9]), while for La^{3+}–Cl^- in molten $LaCl_3$ it is 0.281 nm. This difference corresponds to the difference of the anion sizes; 0.196 nm for Br^- and 0.181 nm for Cl^-. The coordination number of Br^- around La^{3+} was ca. 6 which suggests that molten $LaBr_3$ has an octahedral coordination, like the molten rare earth trichlorides. A second peak, corresponding to Br^-–Br^-, was observed at 0.370 nm as a shoulder. There is no corresponding peak in molten $LaCl_3$. The distance of this is slightly shorter than the expected one 0.415 nm for an octahedron ($r_{Br-Br} = \sqrt{2}\, r_{La-Br}$). This is considered to be due to the poor stability of the octahedra in molten $LaBr_3$ because there are only three Br^- ions per La^{3+} ion. A broad peak in molten $LaBr_3$, which is more

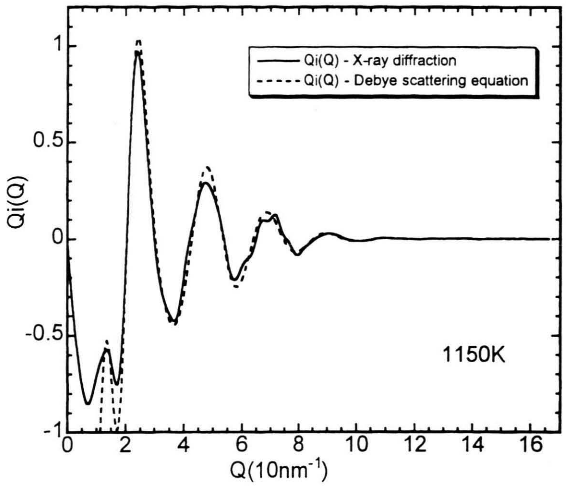

Fig. 3. Reduced intensity function $Q\,i\,(Q)$ of molten $LaBr_3$.

Table 2. Parameters of Debye scattering equation of molten $LaBr_3$ and $LaCl_3$ at 1150 K.

Interaction	n_{ij} (N_{ij})[a]	r_{ij} (nm)	b_{ij} $(10^{-2}$ nm$^2)$
($LaBr_3$)			
Inside the octahedron			
La–Br	12 (6)	0.295	0.045
Br–Br	24 (8)	0.375	0.144
Between the octahedra			
La–La	5 (5)	0.510	0.190
La–Br	24 (12)	0.564	0.324
Br–Br	24 (8)	0.615	0.338
($LaCl_3$)			
Interaction	n_{ij} (N_{ij})[a]	r_{ij} (nm)	b_{ij} $(10^{-2}$ nm$^2)$
Inside the octahedron			
La–Cl	12 (6)	0.281	0.025
Cl–Cl	24 (8)	0.380	0.095
Between the octahedra			
La–La	5 (5)	0.500	0.190
La–Cl	24 (12)	0.552	0.330

[a] N_{ij} is the coordination number of ion j around ion i.

distant by about 0.05 nm than in molten $LaCl_3$, was detected around 0.55 nm. It seems to be due to correlations between the octahedra.

The reduced intensity function $Q\,i\,(Q)$ of molten $LaBr_3$ is shown in Fig. 3, together with the one synthesized from the Debye scattering equation. The experimental line is well reproduced by using the structural parameters listed in Table 2. The parameters for molten $LaCl_3$ are also listed in Table 2. In the analysis of molten $LaBr_3$ it is necessary to assume a Br–Br interaction between the octahedra for obtaining good reproducibility of the $Q\,i\,(Q)$ function, while a corresponding interaction (the second Cl–Cl) does not give a meaningful contribution in case of molten $LaCl_3$. The reason why we obtained the much more distant peak position around 0.55 nm in molten $LaBr_3$ compared with $LaCl_3$ is due to the considerable contribution of the second Br–Br interaction to the functions $Q\,i\,(Q)$ and $G\,(r)$ in addition to the difference in anion size.

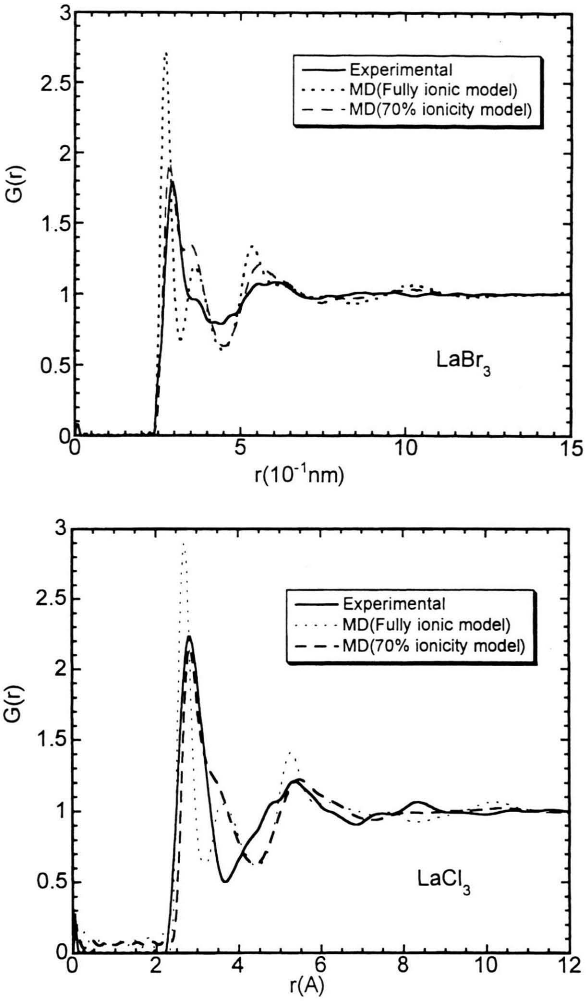

Fig. 4. Correlation functions $G\,(r)$ of molten $LaBr_3$ and $LaCl_3$ by molecular dynamics calculations.

For the MD simulation of molten $LaCl_3$ and $LaBr_3$ the parameters of the pair potentials of (2) were determined to reproduce the function $G\,(r)$. In Figs. 4(a) and (b) the

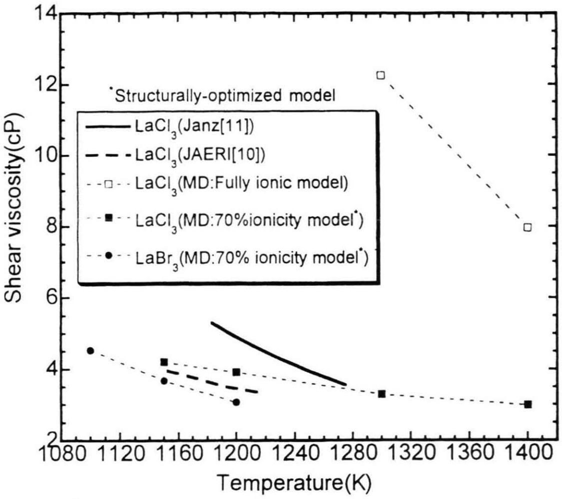

Fig. 5. Shear viscosity of molten $LaBr_3$ and $LaCl_3$.

calculated $G(r)$ functions are plotted. The fully ionic model gave poor agreement with the experimental data while good reproducibility was obtained with the 70% ionicity model for both melts. In [3] it was found that structurally-optimized MD simulations of molten UCl_3 gave dynamic properties which are similar to the experimental ones. Calculated shear viscosities of molten $LaCl_3$ are shown in Fig. 5 together with reported experimental values, the 70% ionicity model showing good agreement. The electric conductivity and shear viscosity of molten $LaBr_3$ were calculated using the MD simulation with the 70% ionicity model. Good agreement with the experimental $G(r)$ function was obtained. The calculated shear viscosity is slightly smaller than that of molten $LaCl_3$. The calculated electric conductivity, 109.957 S/m, is close to the recommended one 114.366 S/m [11]. These calculations suggest that the type of simulation used in the present work anables to predict unknown properties e.g. of molten actinide trihalides.

4. Conclusion

The structures of molten $LaBr_3$ and $LaCl_3$ were investigated by high-temperature XRD measurements. These structures are quite similar. Their difference is ascribed to the difference of size and scattering factor of Br^- and Cl^-. The short range structure of molten $LaBr_3$ is almost the same as that of molten $LaCl_3$.

The shear viscosities of molten $LaBr_3$ and $LaCl_3$ were calculated from structurally-optimized MD calculations. For $LaCl_3$, the 70% ionicity model gave good agreement with the experimental values. In addition, the calculated electric conductivity of molten $LaBr_3$ was found to be almost the same as the recommended one. This suggests that the structurally-optimized simulation is a useful tool for estimating unknown physical properties like in our case the shear viscosity of molten $LaBr_3$.

Acknowledgement

Authors gratefully acknowledges the interest and encouragement of division director Dr. H. Katsuta. The calculations were performed by Fujitsu supercomputer VPP500 at the Japan Atomic Energy Research Institute. Authors also thank Mr. S. Ishizuki for his close cooperation in calculation using the supercomputer.

[1] T. Ogawa, S. Yamagishi, F. Kobayashi, A. Itoh, T. Mukaiyama, M. Handa, and R. G. Haire, Proc. Int. Conf. on Emerging Nuclear Fuel Cycle Systems, Global-'95, 207 (1995).
[2] M. Mizumoto, K. Hasegawa, H. Yokobori, H. Oguri, Y. Okumura, J. Kusano, H. Murata, K. Sakogawa, M. Kawai, T. Nishida, T. Takizuka, and H. Takada, Proc. Int Conf. on Emerging Nuclear Fuel Cycle Systems, Global-'93, 357 (1993).
[3] Y. Okamoto, F. Kobayashi, and T. Ogawa, J. Alloys. Comp. 271–273, 355 (1998).
[4] H. Ohno, K. Igarashi, N. Umesaki, and K. Furukawa, Molten Salt Forum vol. 3, Trans Tech Publications, Switzerland 1994.
[5] K. Kawamura, Molecular Dynamics Simulations, ed. F. Yonezawa, Springer-Verlag, New York, 1992.
[6] Y. Okamoto, H. Hayashi, and T. Ogawa, J. Nucl. Mater. **247,** 86 (1997)
[7] Y. Kataoka, Bull. Chem. Soc. Japan **62,** 1421 (1989).
[8] M.-L. Saboungi, D. L. Price, C. Scamehorn, and M. P. Tosi, Europhys. Lett. **15,** 283 (1991).
[9] K. Kramer, T. Schleid, M. Schulze, W. Urland, and G. Meyer, Z. Anorg. Allg. Chem. **575,** 61 (1989).
[10] H. Hayashi, Y. Okamoto, T. Ogawa, Y. Sato, and T. Yamamura, MS-5 conference, Dresden, Germany August 1997.
[11] G. J. Janz, J. Phys. Chem. Ref. Data **17,** 1 (1998).